Emergent Materials (2019) 2:363–370
https://doi.org/10.1007/s42247-019-00057-1

ORIGINAL ARTICLE

Effect of preparation method on the properties of poly(methyl methacrylate)/mesoporous silica composites

M. A. Sibeko[1] · M. L. Saladino[2] · F. Armetta[2] · A. Spinella[3] · A. S. Luyt[4]

Received: 6 March 2019 / Accepted: 13 September 2019 / Published online: 6 November 2019

Abstract

The preparation method of a polymer composite and the filler loading are amongst the factors that influence the properties of the final composites. This article studies the effect of these factors on the thermal stability and thermal degradation kinetics of poly(methyl methacrylate) (PMMA)/mesoporous silica (MCM-41) composites filled with small amounts of MCM-41. The PMMA/MCM-41 composites were prepared through in situ polymerisation and melt mixing methods, with MCM-41 loadings of 0.1, 0.3, and 0.5 wt.%. The presence of MCM-41 increased the thermal stability of PMMA/MCM-41 composites prepared by melt mixing, but in the case of the in situ polymerised samples, the MCM-41 accelerated the degradation of the polymer. As a result, the activation energy was low and less energy was required to initiate and propagate the degradation process of these composites. The small-angle X-ray scattering (SAXS) measurements showed that the preparation method of the composites had no influence on the pore size of MCM-41, but the PMMAs used in the two methods both had shorter chains than the MCM-41 pore size. This allowed the polymer chains to be trapped inside the pores of the filler and be immobilised, as was observed from nuclear magnetic resonance (NMR) spectroscopy. The immobilisation of the polymer chains was more significant in the in situ polymerised samples.

Keywords Poly(methyl methacrylate) (PMMA) · Mesoporous silica (MCM-41) · In situ polymerisation · Melt mixing · Thermal degradation kinetics · ^{13}C {^{1}H} CP-MAS-NMR

1 Introduction

Organic–inorganic hybrid materials, especially polymer matrices with inorganic nanoscale building blocks, have drawn extensive attention of researchers, mostly because they combine superior mechanical and thermal properties of inorganic phases with the flexibility and processability of organic polymers [1, 2]. The comprehensive performance of these composites depends on many factors, such as the intrinsic properties of the polymers, the preparation method of the composites, the dispersion of the nanoparticles in the polymer matrix, and the interfacial compatibility between the nanoparticles and the polymer matrix. Amongst the well-studied nanoscale materials such as nanoclays, nanofibers, and carbon nanotubes, mesoporous molecular sieves are a new class of nanoscale materials which possess large surface areas and tuneable pore sizes between 2 and 50 nm [3–6]. Mesoporous silicas have different pore sizes and structures which can be differentiated into hexagonal mesoporous silica (MCM-41), cubic MCM-48, hexagonal SBA-15, wormhole framework MSU-J, hexagonally ordered MSU-H, and mesocellular silica foam MSU-H [7–9].

Although mesoporous molecular sieves have been widely used in other applications, their use as polymer additives has attracted less attention. Only recently, nano-mesoporous silica has been used as an additive with the goal of enhancing the mechanical and thermal properties of polymers. The pores on the surface of the silica provide the possibility of incorporating diverse organic guest species, including polymers, into their

✉ A. S. Luyt
aluyt@qu.edu.qa

[1] Department of Chemistry, University of the Free State (Qwaqwa Campus), Private Bag X13, Phuthaditjhaba 9866, South Africa

[2] Dipartimento Scienze e Tecnologie Biologiche, Chimiche e Farmaceutiche – STEBICEF and INSTM UdR – Palermo, Università di Palermo, Viale delle Scienze pad.17, I-90128 Palermo, Italy

[3] ATeN Center, Università di Palermo, Via F. Marini 14, I-90128 Palermo, Italy

[4] Center for Advanced Materials, Qatar University, PO Box 2713, Doha, Qatar

ordered mesoporous structures [4–6]. A polymer can be introduced inside the mesopores by melt compounding or through in situ polymerisation of organic monomers, depending on the mesoporous size, the molecular weight, the structure of the polymer, and the physical or chemical interactions. The microstructure of the interface between the matrix and pore openings of the fillers can be easily tailored. It has been reported that the polymer in the nano-sized pores, extending along the channels to the openings, can not only enhance the miscibility through entanglement and inter-diffusion between the matrix and the particulate, but can also strongly supress the aggregation of the fillers [9–12].

Only a few studies reported on the improvement of poly(methyl methacrylate) (PMMA) properties with the addition of mesoporous silica, prepared through different polymerisation methods [6, 8, 13]. Run et al. [14] prepared PMMA/mesoporous molecular sieve (MMS) composites by an in situ polymerisation method with filler contents of 2 and 10 wt.%. An increase in thermal stability and glass transition temperature of PMMA was observed with an increase in MMS loading. The elevated decomposition temperature of PMMA was attributed to the strong interaction between the MMS particles and the matrix. Zhang et al. [15] evaluated the effect of MSU-F silica at 5 and 10 wt.% loading on the thermal and mechanical properties of PMMA. The composites were prepared through batch emulsion polymerisation and compression moulding. The degradation of PMMA occurred in two degradation steps: the first step was attributed to the unzipping of chains starting at both the vinylidene end groups and the weak head-to-head linkages, while the second step was associated with chains undergoing degradation through random chain scission. The PMMA/MSU-F composites displayed mainly the second decomposition stage, as the presence of silica reduced the vinylidene end group and head-to-head linkages. However, the thermal stability of PMMA increased with increasing MSU-F content, which was attributed to the radical scavenging role of the silica and the intrinsic stiffening of the polymer chains. Mohammadnezhad et al. [16] incorporated PMMA into amine-functionalised MCM-41 by ultrasonic irradiation. The thermal stability of PMMA increased by 50 °C with the addition of 2 wt.% MCM-41, which was associated with the improvement in the interfacial interaction between the two components.

So far, all the papers in the literature relating to PMMA/MCM-41 composites were focused on the effect of MCM-41 at high contents, ranging from 1 to 10 wt.% [6, 8, 14, 15], on the thermal properties of PMMA. This motivated this study where we evaluated the influence of lower MCM-41 contents on the properties of PMMA. To the best of our knowledge, there is no study that compared the effect of MCM-41 at low content (0.1–0.5 wt.%) and prepared through different methods, on the structure, thermal stability, and degradation kinetics of PMMA. This paper reports on these factors, where the structures of the composites were investigated through small-angle X-ray scattering (SAXS). ^{13}C cross-polarisation magic-angle spinning nuclear magnetic resonance (^{13}C $\{^{1}H\}$ CP-MAS NMR) spectroscopy measurements were carried out to investigate the interaction between the PMMA and the MCM-41, and thermogravimetric analysis (TGA) was used to study the thermal stability and thermal degradation kinetics of the composites. The results obtained in this study are compared with those reported on PMMA/MCM-41 composites prepared by melt mixing [17].

2 Materials and methods

2.1 Materials

All the reagents were purchased from Sigma Aldrich. Methyl methacrylate (MMA, 99%) was purified using a disposable column to eliminate the hydroquinone monomethyl ether as stabiliser. 2,2-Diethoxyacetophenone (95%, density of 1.034 g/mL at 25 °C) and MCM-41 (surface area ~ 1000 m^2 g^{-1}, pore sizes ranging between 2.1 and 2.7 nm, pore volume 0.98 cm^3 g^{-1}) were used as received.

2.2 Preparation of the PMMA/MCM-41 composites

The PMMA/MCM-41 composites were prepared by an in situ polymerisation method following the procedure already described by Saladino et al. [18]. MCM-41 powder was dispersed by ultrasonication into the methyl methacrylate (MMA) monomer at different contents (0.1, 0.3, and 0.5 wt.%) for 10 min. 2,2-Diethoxyacetophenone was then added to start the photo-curing process. The vials containing the samples were irradiated at 365 nm in a Rayonet reactor equipped with eight 35-W Hg lamps for at least 3 h, up to complete photo-curing. The obtained PMMA had a molecular weight distribution of 600–3000 g mol^{-1} determined by size exclusion chromatography-MALDI-TOF mass spectrometry. The transparent composites (loaded with 0.1, 0.3, and 0.5 wt.% of MCM-41) were cut and lapped to obtain discs of 1 cm in diameter and 2 mm in thickness. Neat PMMA was also prepared following the same procedure. The preparation procedure for PMMA/MCM-41 composites through melt mixing was reported in a previous paper [17].

2.3 Characterisation techniques

The thermogravimetric (TGA) analyses were carried out in a Perkin Elmer STA6000 simultaneous thermal analyser. The thermal stability was evaluated by heating samples, with masses ranging between 20 and 25 mg, from 30 to 600 °C at a heating rate of 10 °C min^{-1} under nitrogen flow (20 mL min^{-1}). The same instrument was used to analyse

the thermal degradation behaviour of the samples over the same temperature range. The thermal degradation kinetics studies were performed at heating rates of 3, 5, 7, and 9 °C min^{-1} under a nitrogen flow of 20 mL min^{-1}. The plots of ln β vs. 1/T were obtained from the TGA curves recorded at several heating rates (Eq. (1)). The plots are shown in Figs. 2 and 3.

$$In\ \beta = -1.052\left(\frac{E_a}{RT}\right) + c \quad (1)$$

where β is the heating rate in °C min^{-1}, c is the intercept, E_α is the activation energy in kJ mol^{-1}, R is the universal gas constant (8.314 J K^{-1} mol^{-1}), and T is the temperature in Kelvin.

SAXS measurements were done by using a Bruker AXS Nanostar-U instrument which had a Cu rotating anode source working at 40 kV and 18 mA. The operational conditions used in the analysis were followed as described in a previous paper [17]. The ^{13}C $\{^1H\}$ CP-MAS NMR spectra were obtained at room temperature using a Bruker Avance II 400 MHz (9.4 T). The proton ($T_{1\rho}(H)$) and carbon ($T_{1\rho}(C)$) spin–lattice relaxation times in the rotating frame were also determined following the conditions and procedure described in a previous paper [17].

3 Results and discussion

3.1 Thermogravimetric analysis and thermal degradation kinetics

The TGA curves of PMMA and PMMA/MCM-41 composites are reported in Fig. 1 and summarised in Table 1. The thermal stability of PMMA has been well studied, and it was established that its thermal stability or degradation mechanism depends on several factors, one of which is the polymerisation method. It is believed that PMMA polymerised through free

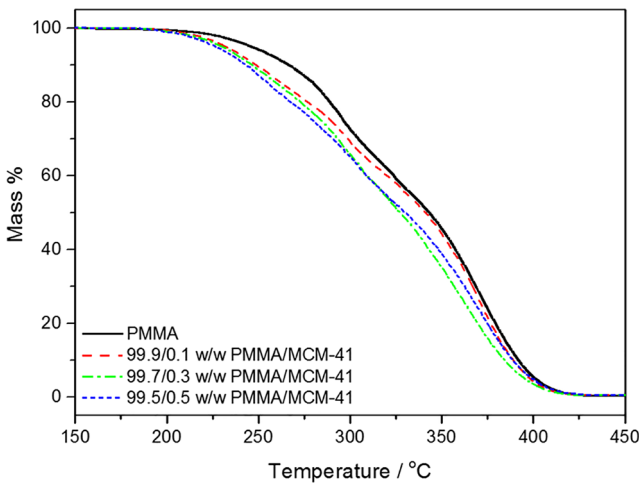

Fig. 1 TGA curves of PMMA and PMMA/MCM-41 composites

Table 1 TGA results for PMMA and the PMMA/MCM-41 composites

Samples	T_{20}/°C	T_{60}/°C	% Residue
PMMA	288.9	368.1	–
99.9/0.1 *w/w* PMMA/MCM-41	275.4	366.4	–
99.7/0.3 *w/w* PMMA/MCM-41	272.2	356.1	0.4
99.5/0.5 *w/w* PMMA/MCM-41	267.3	362.1	0.7

T_{20} and T_{60}, the temperatures at 20 and 60% mass loss

radical polymerisation has poor thermal stability, which is mainly due to the presence of polymer chains with different structures. Cao et al. [19] reported three degradation steps for PMMA polymerised through free radical polymerisation. The first step was attributed to degradation initiated by the scission of chains containing head-to-head (H-H) linkages, and this was observed between 150 and 230 °C. The second step between 230 and 300 °C was associated with the degradation of chains having unsaturated ends, while the third step between 310 and 420 °C was ascribed to chains undergoing degradation initiated by random chain scission. Polymer chains with head-to-head linkages or unsaturated ends are thermally unstable, and they normally initiate chains with weak links to decompose into MMA monomers below 300 °C through unzipping reactions. PMMA that is stable below 300 °C can be produced by using anionic polymerisation, which shows only one degradation step starting around 360 °C [20]. The TGA curves of PMMA and the PMMA/MCM-41 composites illustrated in Fig. 1 show the three degradation steps described above, indicating that the in situ polymerisation followed a free radical route in our case. This is contrary to the degradation curves we obtained for our melt mixed samples [17], where only one degradation step was observed for the neat polymer and the nanocomposites. The polymer in this case was obviously prepared through anionic polymerisation.

Figure 1 clearly shows that the addition of and increase in MCM-41 loading decreased the thermal stability of PMMA. The presence of MCM-41 obviously accelerated the degradation of PMMA. Mesoporous molecular sieves had been identified as catalysts with large pore sizes between 2 and 50 nm. However, there are conflicting reports as to whether or not MCM-41 can act as an active catalyst. Additional catalytic functions can be introduced by incorporating different metals or metal oxides into the MCM-41 structure. In several studies, aluminium sources were incorporated into the framework of MCM-41 to produce acidic properties [21, 22]. Obali et al. [21] investigated the influence of an acidic MCM-41 aluminosilicate catalyst on the degradation of polypropylene (PP). Mesoporous aluminosilicate samples were prepared from different aluminium sources, and a neat MCM-41 catalyst was also used as a reference material. It was reported that MCM-41 did not have a significant influence on the thermal stability of PP, but a significant decrease (~ 100 °C) in thermal stability

was observed in the presence of the aluminosilicate catalysts. The same catalytic effect of a mesoporous sol–gel Al-MCM-41 catalyst was also reported by Saha et al. [22] in the case of LDPE. In our case, the trapping of the in situ polymerised chains in the MCM-41 pores probably improved the absorption of heat energy by the chains, which more effectively initiated the polymer degradation process. In our previous work, we found that the thermal stability of PMMA/MCM-41 composites prepared by melt mixing increased in the presence of MCM-41, which was attributed to the well dispersed MCM-41 that might have trapped the free radical chains and the volatile degradation products, so that higher temperatures were needed to provide enough energy for the propagation of the degradation process, and for the release of the volatile degradation products [17]. The polymer was prepared by anionic polymerisation and was stable up to 368 °C. The different morphology of the in situ prepared PMMA, as well as its lower thermal stability, most probably caused the decreasing thermal stability with increasing MCM-41 content in the samples (Fig. 1). Since the MCM-41 was present during the polymerisation process, the entrapment of the polymer chains in the MCM-41 pores and the interaction between these chains and the MCM-41 particles were probably different from those observed in the melt mixed samples [17], causing the observed decreasing thermal stability.

The thermal degradation kinetics of polymers has been extensively studied in literature, using mostly TGA. In these kinetic studies, the mass loss of the sample is continuously recorded as a function of temperature at several heating rates. Isoconversional methods are generally used to determine the activation energy from the reciprocal temperature and fraction of conversion obtained from TGA experiments at differing heating rates [23]. The activation energy is defined as the amount of energy that is required by a material to initiate the degradation process. The isoconversional graphs of ln β versus 1/T shown in Figs. 2 and 3 were obtained from the TGA curves after analysis at heating rates of 3, 5, 7, and 9 °C min^{-1}. The activation energy (E_a) values were calculated from the slopes of the isoconversional plots according to Eq. (1).

The relationship between the activation energies and the extent of mass loss for PMMA and the PMMA/MCM-41 composites is illustrated in Fig. 4. Generally, the activation energy of PMMA and the PMMA/MCM-41 composites increased continuously as the extent of mass loss increased. The dependence of E_a on the extent of degradation usually means that the degradation mechanism of the polymer changed during the degradation process and occurred in multiple steps. Some authors attributed this trend to a change in reaction order, which may have been brought about by a change in the degradation mechanism from a first order unzipping reaction to a higher order chain scission reaction [24]. In the case of the melt mixed samples, there was an initial increase in activation energy at low mass loss, which flattened off at

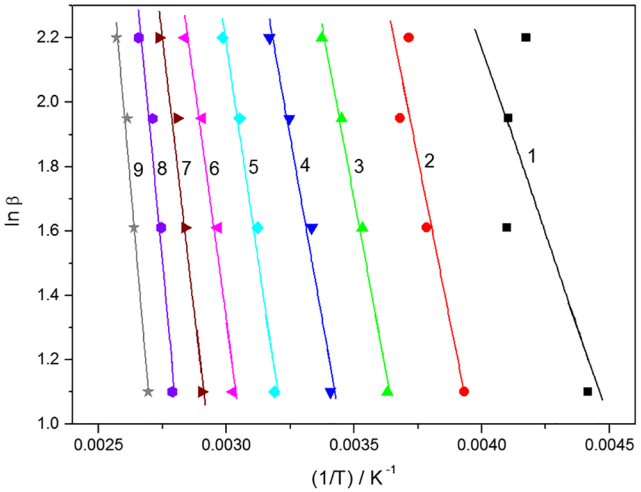

Fig. 2 Ozawa–Flynn-Wall plots for PMMA for the following degrees of conversion: (1) α = 0.1, (2) α = 0.2, (3) α = 0.3, (4) α = 0.4, (5) α = 0.5, (6) α = 0.6, (7) α = 0.7, (8) α = 0.8, (9) α = 0.9

higher extents of mass loss. The initial increase in E_a was attributed to the trapping by the filler of the volatile degradation products formed during the initial stages of degradation, which was released later as the degradation proceeded [17]. It was assumed that there was no change in the degradation mechanism, but rather an immobilisation of the free radical chains and trapping of the volatile degradation products by the porous filler. However, although there also seems to be immobilisation of free radical chains and trapping of volatile degradation products by the porous filler in the case of the in situ polymerised samples, as discussed later on in this paper, the continuous increase in activation energy with increase in the extent of mass loss for the in situ polymerised samples probably points to the multiple step degradation process observed in Fig. 1.

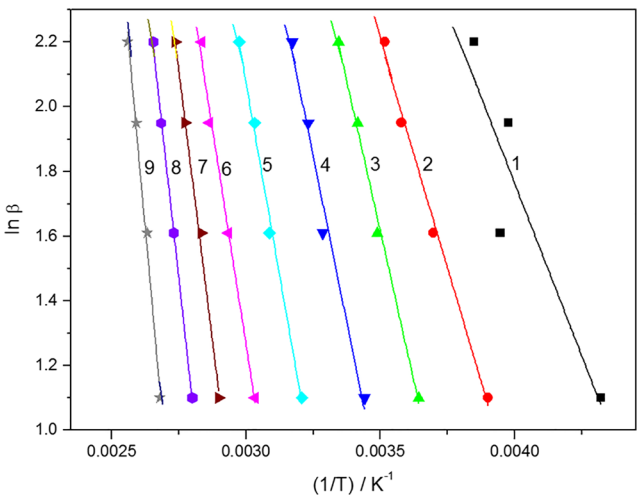

Fig. 3 Ozawa–Flynn-Wall plots for PMMA/MCM-41 for the following degrees of conversion: (1) α = 0.1, (2) α = 0.2, (3) α = 0.3, (4) α = 0.4, (5) α = 0.5, (6) α = 0.6, (7) α = 0.7, (8) α = 0.8, (9) α = 0.9

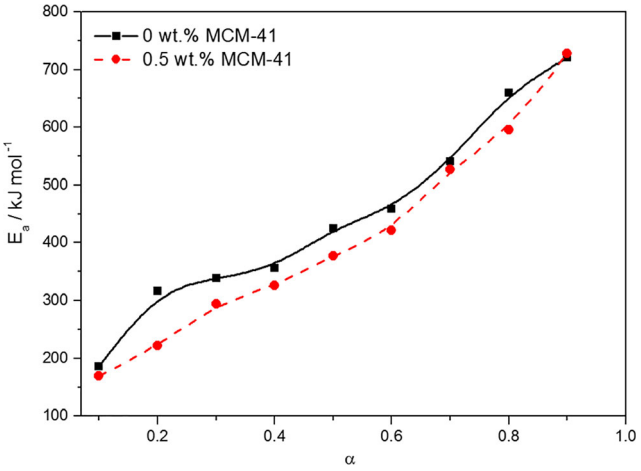

Fig. 4 Activation energy vs. extent of degradation for PMMA and PMMA/MCM-41 composites with 0.5 wt.% MCM-41

Figure 4 also shows that the PMMA/MCM-41composites have lower activation energies than the neat PMMA. This can be attributed to the catalytic effect of the filler, which probably increased the initiation rate through the trapping of the polymer chains in the MCM-41 pores. Araujo et al. [25] reported a similar catalytic effect of MCM-41, where they observed that the activation energy of poly(ethylene terephthalate) (PET) decreased from 231 to 195 kJ mol^{-1} in the presence of MCM-41. For our previously reported melt mixed samples [17], the activation energy values of the composites at 0.5 wt.% were found to be significantly higher than those of the neat PMMA. Furthermore, the activation energy of the PMMA/MCM-41 (0.5 wt.%) at 10% conversion for the in situ polymerised sample was 168.9 kJ mol^{-1}, while for the melt mixed samples, the activation energy was 585.8 kJ mol^{-1}. This implied that more energy was required to initiate and propagate the degradation of the composites prepared by melt mixing, which is also in line with the higher thermal stability of the composites observed from the TGA curves.

3.2 Small-angle X-ray scattering

SAXS measurements were done to investigate if the polymer changed the structure of the mesoporous MCM-41. Measurements taken from different portions of a sample looked similar, which proved that the samples were homogenous. Figure 5 shows the SAXS pattern of PMMA, MCM-41, and the PMMA/MCM-41 composites after background and thickness corrections. PMMA is an amorphous polymer, and as expected, its SAXS pattern does not display any peak in the investigated scattering intensity *I(Q)* range. As for the SAXS pattern of MCM-41, a high-intensity peak at 0.15 Å^{-1} (100) and two low-intensity reflections ((110) and (200)) were observed, which correspond to the typical hexagonal structure of MCM-41 [25].

The SAXS patterns of the PMMA/MCM-41 composite containing 0.1 wt.% do not show any characteristic peaks of the MCM-41, probably due to the very low amount of the MCM-41 in the sample. The characteristic peaks of MCM-41 in the PMMA/MCM-41 composites started to appear for the sample containing 0.3 wt.% MCM-41, and their intensity increased as the MCM-41 loading increased. In both samples, the MCM-41 maintained its hexagonal lattice symmetry after composite formation. The distance between the centre of two adjacent pores in the hexagonal structure of MCM-41 is usually correlated with the interplanar distance, which can be obtained from the position of the (100) peak in the SAXS pattern [21]. It has been reported that in the presence of the polymer, the (100) peak shifted to smaller angles, indicating that the interplanar distance and the distance between the centre of two adjacent pores in the MCM-41 have increased. As shown in Fig. 5, there is no shift in the (100) peak in the case of PMMA/MCM-41 composites, demonstrating that the porous size of the mesoporous materials did not change after the composite formation. The polymer chains were probably trapped in the pores of the filler without influencing the interplanar distance of the filler.

To investigate the probability of the polymer chains entering the pores of MCM-41, the radius of gyration of the polymer chains has been calculated by using Eq. (2) [8].

$$R_g^2 = \frac{nl^2}{6} \tag{2}$$

in which n represents the number of monomer units in a polymer chain and l represents the length of the monomer unit. The length of the monomer unit used in the calculation of radius of gyration was 1.54 Å. The polymerised PMMA had a molecular weight range from 600 to 3000 g mol^{-1}, and these average values were used to calculate the radius of gyration, which gave values between 0.15 and 0.30 nm. These values are significantly smaller than the pore size of the MCM-41, which ranged between 2.1 and 2.7 nm. We can therefore conclude that there was a possibility of the polymer chains to penetrate the MCM-41 pores during composite preparation. Even though there was no change in pore size of MCM-41 as observed by SAXS analysis, it is possible that the polymer was polymerised inside the pores of the filler without changing its size. Similarly, there was no change in the pore size of MCM-41 in the PMMA/MCM-41 composites prepared by the melt mixing method [17].

3.3 ^{13}C cross-polarisation magic-angle spinning nuclear magnetic resonance (^{13}C {^{1}H} CP-MAS-NMR) spectroscopy

The ^{13}C {^{1}H} CP-MAS NMR spectra of PMMA and PMMA/MCM-41 composite filled with 0.5 wt.% MCM-41

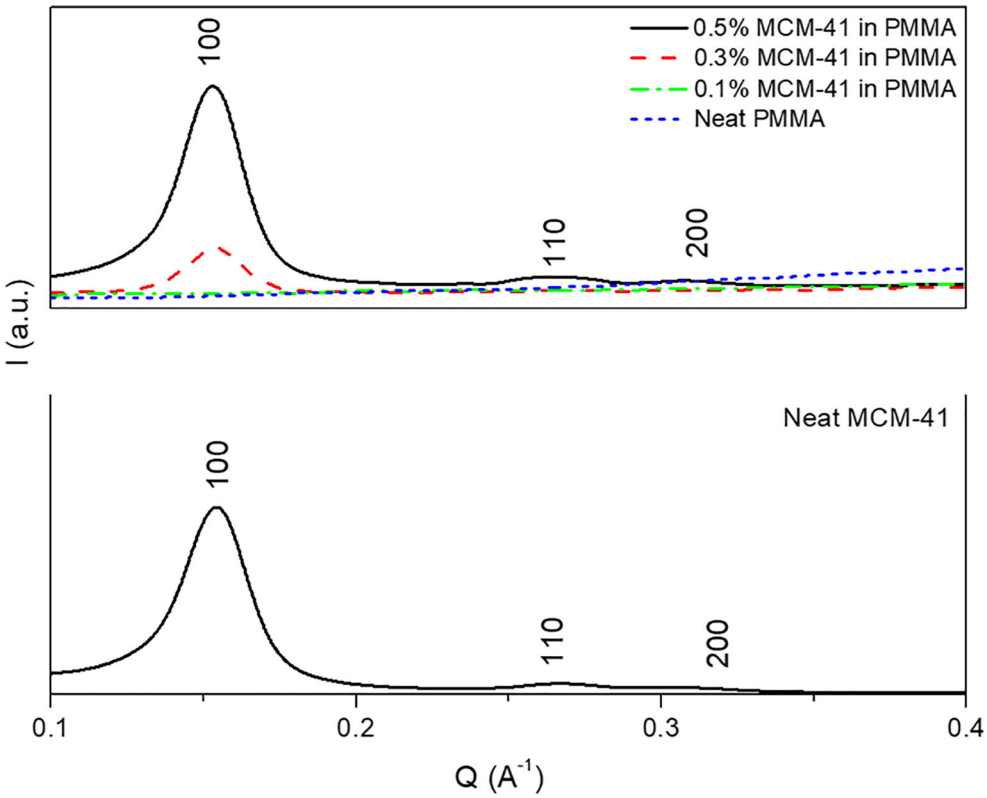

Fig. 5 SAXS intensities vs. scattering vector Q of PMMA/MCM-41 composites and MCM-41

are shown in Fig. 6. The spectrum of PMMA shows five resonances at 177.9, 55.4, 52.3, 45.2, and 16.6 ppm, which are attributed to the carbonyl carbon, methoxy group, quaternary carbon of the polymer chain, and methylene and methyl groups respectively. There was no change in the chemical shift and in the signal shape of PMMA in the presence of MCM-41.

The relaxation processes were determined to investigate the possible interaction between the MCM-41 and the polymer. The proton ($T_{1\rho}$(H)) and carbon ($T_{1\rho}$(C)) spin–lattice relaxation times were acquired to evaluate the dynamic changes in the PMMA as a result of MCM-41 addition. The $T_{1\rho}$(H) and $T_{1\rho}$(C) relaxation time values for pure PMMA and the

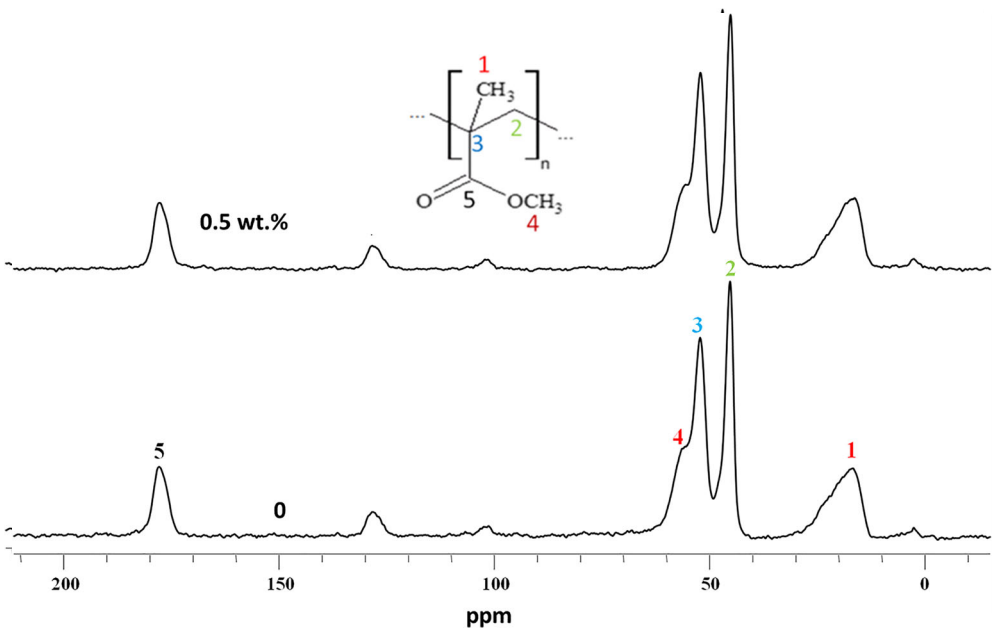

Fig. 6 ^{13}C {^{1}H} CP-MAS NMR spectra of PMMA and of the 0.5% PMMA/MCM-41 composite

Table 2 Relaxation time values for all the peaks in the ^{13}C spectra of PMMA and the PMMA/MCM-41 composites with 0.5 wt.% of MCM-41

Signal (ppm)	PMMA		PMMA/MCM-41	
	$T_{1\rho}H$ (ms)	$T_{1\rho}C$ (ms)	$T_{1\rho}H$ (ms)	$i_{1\rho}C$ (ms)
5 (177.9)	14.3 ± 0.2	48.4 ± 0.2	40.8 ± 0.2	64.7 ± 0.2
4 (55.4)	–	24.3 ± 0.3	45.0 ± 0.2	29.8 ± 0.2
3 (52.3)	20.5 ± 0.1	42.7 ± 0.2	42.7 ± 0.2	57.9 ± 0.3
2 (45.2)	13.4 ± 0.1	63.6 ± 0.1	34.4 ± 0.1	89.2 ± 0.3
1 (16.6)	15.2 ± 0.2	20.8 ± 0.2	25.6 ± 0.2	18.4 ± 0.2

PMMA/MCM-41 composite loaded with 0.5 wt% MCM-41 obtained from each peak in the ^{13}C spectra are reported in Table 2. There is a significant increase in $T_{1\rho}(H)$ values of the carbon nuclei of PMMA in the presence of MCM-41. The $T_{1\rho}(C)$ values of all the carbons increased in the presence of MCM-41, but not that of the methyl group (1). The increase in the $T_{1\rho}(C)$ values implies that the main chain motions were hindered by the presence of MCM-41. The addition of 0.5 wt.% MCM-41 in PMMA/MCM-41 composites prepared by melt mixing showed no significant influence on the $T_{1\rho}(H)$ relaxation time value, while an increase in $T_{1\rho}(C)$ was only observed for the methylene and carbonyl carbon. During in situ polymerisation, it is possible that more polymer chains get polymerised inside the MCM-41 pores, which causes more polymer chains being trapped inside the pores, resulting in effective restriction of the polymer chains and an increase in the relaxation times compared with the melt mixed samples [17]. The decrease in the mobility of the polymer chains can also be attributed to chemical-physical interactions involving functional groups of the polymer chain like silanol groups (Si–OH) on the MCM-41 surface, which can form hydrogen bonding interactions with the carbonyl groups on the PMMA chains.

4 Conclusions

The aim of the work reported in this article was to investigate the effect of preparation method of PMMA/MCM-41 composites and loading of MCM-41 on the thermal stability and thermal degradation kinetics of PMMA. The properties of the PMMA/MCM-41 composites prepared by the in situ polymerisation method were compared with those prepared by melt mixing with the same filler loading. The presence of MCM-41 had different effects on the thermal stability of the PMMA in the PMMA/MCM-41 composites prepared by the two methods. An increase in thermal stability was observed for the composites prepared by melt mixing, while a decrease was observed for the composites prepared by in situ polymerisation, due to the catalytic behaviour of the MCM-41, which was probably the result of the confinement of the polymer chains in the MCM-41 pores and the interaction between the PMMA and MCM-41, as was confirmed by ^{13}C cross-polarisation magic-angle spinning nuclear magnetic resonance (^{13}C $\{^{1}H\}$ CP-MAS-NMR) spectroscopy analysis, and which resulted in the immobilisation of the polymer chains, as was also confirmed by NMR. One other factor that was not taken into account and might have contributed to the decrease in the thermal stability of the composites is the polymerization method of the PMMA.

Acknowledgements The authors acknowledge the University of Palermo for supporting this research through the CORI2013 (Bando per la concessione di contributi per l'avvio e lo sviluppo di collaborazioni dell'Ateneo 2013—Azione D—prot. 32827 del 2/5/2013).

The authors would like to thank Dr. Ivana Pibiri of University of Palermo, STEBICEF Department, for the use of the Rayonet reactor.

NMR and SAXS experimental data were provided by ATeN Center—Università di Palermo (http://www.atencenter.com).

Funding information Open Access funding provided by the Qatar National Library. The National Research Foundation of South Africa provided the bursary funding which enabled the student to do the research presented in this paper. The publication of this article was funded by the Qatar National Library.

Data availability The raw/processed data required to reproduce these findings cannot be shared at this time as the data also forms part of an ongoing study.

Compliance with ethical standards

Conflict of interest The authors declare that they have no conflict of interest.

References

1. H. Wang, S. Meng, P. Xu, W. Zhong, Q. Du, Effect of traces of inorganic content on thermal stability of poly (methyl methacrylate) nanocomposites. Polym. Eng. Sci. **47**, 302–307 (2007). https://doi.org/10.1002/pen.20708
2. C.B. Yu, C. Wei, J. Lv, H.X. Liu, L.T. Meng, Preparation and thermal properties of mesoporous silica/phenolic resin nanocomposites via in situ polymerization. eXPRESS Polymers Letters **6**, 783–793 (2012). https://doi.org/10.3144/expresspolymlett.2012.84
3. A. Jomekian, M. Pakizeh, A.R. Shafiee, S.A.A. Mansoori, Fabrication or preparation and characterization of new modified MCM-41/PSf nanocomposite membrane coated by PDMS. Sep. Purif. Technol. **80**, 556–565 (2011). https://doi.org/10.1016/j.seppur.2011.06.011

4. S. Storck, H. Bretinger, W.F. Maier, Characterization of micro- and mesoporous solids by physisorption methods and pores-size analysis. Appl. Catal. A Gen. **174**, 137–146 (1998)
5. F.A. Zhang, M. Luo, Z.J. Chen, Z.B. Wei, T.J. Pinnavaia, Effect of mesoporous silica particles on the emulsion polymerization of methyl methacrylate. Polym. Eng. Sci. **54**, 2746–2752 (2013). https://doi.org/10.1002/pen.23830
6. L.D. Perez, L.F. Giraldo, W. Brostow, B.L. Lopez, Poly (methyl acrylate) plus mesoporous silica nanohybrids: mechanical and thermophysical properties. e-Polymers **7**, 324–334 (2007). https://doi.org/10.1515/epoly.2007.7.1.324
7. N. Wang, N. Gao, S. Jiang, Q. Fang, E. Chen, Effect of different MCM-41 fillers with PP-g-MA on mechanical and crystallization performance of polypropylene. Compos. Part B **42**, 1571–1577 (2011). https://doi.org/10.1016/j.compositesb.2011.04.012
8. F.A. Zhang, D.K. Lee, T.J. Pinnavaia, PMMA/mesoporous silica nanocomposites: effect of framework structure and pore size on thermomechanical properties. Polym. Chem. **1**, 107–113 (2010). https://doi.org/10.1039/b9py00232d
9. N. Wang, H. Li, J. Zhang, Polymer-filled porous MCM-41: an effective means to design polymer-based nanocomposites. Mater. Lett. **59**, 2685–2688 (2005). https://doi.org/10.1016/j.matlet.2005.04.020
10. N. Wang, Y. Shao, Z. Shi, J. Zhang, H. Li, Preparation and characterization of epoxy composites filled with functionalized nano-sized MCM-41 particles. J. Mater. Sci. **43**, 3683–3688 (2008). https://doi.org/10.1007/s10853-008-2591-4
11. N. Wang, Y. Shao, Z. Shi, J. Zhang, H. Li, Influence of MCM-41 particle on mechanical and morphological behavior of polypropylene. Mater. Sci. Eng. A **497**, 363–368 (2008). https://doi.org/10.1016/j.msea.2008.07.019
12. N. Wang, Q, Fang, Y. Shao, J. Zhang. Microstructure and properties of polypropylene composites filled with co-incorporation of MCM-41 (with template) and OMMT nanoparticles prepared by melt-compounding. Mater. Sci. Eng. A 2009; 512:32–38. DOI: https://doi.org/10.1016/j.msea.2009.01.027
13. F.A. Zhang, C. Song, C.L. Yu, Effect of preparation methods on the property of PMMA/SBA-15 mesoporous silica composites. J. Polym. Res. **18**, 1757–1764 (2011). https://doi.org/10.1007/s10965-011-9582-x
14. M.T. Run, S.Z. Wu, D.Y. Zhang, G. Wu, A polymer/mesoporous molecular sieve composite: preparation structure and properties. Mater. Chem. Phys. **105**, 341–347 (2007). https://doi.org/10.1016/j.matchemphys.2007.04.070
15. F.A. Zhang, D.K. Lee, T.J. Pinnavaia, PMMA-mesocellular foam silica nanocomposites prepared through batch emulsion polymerization and compression molding. Polymer **50**, 4768–4774 (2009). https://doi.org/10.1016/j.polymer.2009.08.007
16. G. Mohammadnezhad, S. Abad, R. Soltani, M. Dinari, Study on thermal, mechanical and adsorption properties of amine-functionalized MCM-41/PMMA and MCM-41/PS nanocomposites prepared by ultrasonic irradiation. Ultrasonic- Sonochemistry **39**, 765–773 (2017). https://doi.org/10.1016/j.ultsonch.2017.06.001
17. M.A. Sibeko, A.S. Luyt, M.L. Saladino, E. Caponetti, Morphology, mechanical and thermal properties of poly(methyl methacrylate) (PMMA) filled with mesoporous silica (MCM-41) prepared by melt compounding. J. Mater. Sci. **51**, 3957–3970 (2016). https://doi.org/10.1007/s10853-015-9714-5
18. M.L. Saladino, A. Zanotto, D. Chillura Martino, A. Spinella, G. Nasillo, E. Caponetti, Ce:YAG nanoparticles embedded in a PMMA matrix: preparation and characterization. Langmuir. **26**, 13442–13449 (2010)
19. C. Cao, Z. Tan, S. Sun, Z. Liu, H. Zhang, Enhancing the thermal stability of poly (methyl methacrylate) by removing the chains with weak links in a continuous polymerization. Polym. Degrad. Stab. **96**, 2209–2214 (2011). https://doi.org/10.1016/j.polymdegradstab.2011.09.005
20. I. Popovic, L. Katsikas, The thermal degradation of some polymeric di-alkyl esters of itaconic acid. Journal of Serbian Chemical Society **78**, 2179–2200 (2013)
21. Z. Obali, N.A. Sezgi, T. Dogu, Performance of acidic MCM-41-like aluminosilicate catalysts in pyrolysis of polypropylene. Chem. Eng. Commun. **196**, 116–130 (2009)
22. W. Saha, A.C.K.C.P.K. Reddy, A.K. Choshal, in *Proceedings of the National Conference on Frontiers in Chemical Engineering*. Effect of aluminium content in Al-MCM-41 catalyst on decomposition of low-density polyethylene (LDPE), pp. NCFCE–N2007
23. J.H.J. Flynn, The Isoconversional method for determination of energy of activation at constant heating rates. J. Therm. Anal. **27**, 95–102 (1983). https://doi.org/10.1007/BF01907325
24. Z. Gao, T. Kaneko, D. Hou, M. Nakada, Kinetics of thermal degradation of poly (methyl methacrylate) studied with the assistance of the fractional conversion at the maximum reaction rate. Polym. Degrad. Stab. **84**, 399–403 (2004). https://doi.org/10.1016/j.polymdegradstab.2003.11.015
25. S.A. Araujo, A.S. Araujo, N.S. Fernandes, V.J. Fernandes Jr., M. Ionashiro, Effect of the catalyst MCM-41 on the kinetic of the thermal decomposition of poly (ethylene terephthalate). J. Therm. Anal. Calorim. **99**, 465–469 (2010). https://doi.org/10.1007/s10973-009-0490-9